INAF/OATs
LFI Project System Team

Planck LFI

TITLE: **PLANCK/LFI: Potential telemetry saving on HFI 4K high resolution thermometers, LFI constraints**

DOC. TYPE: Technical Note
PROJECT REF.: PL-LFI-OAT-TN-064 PAGE: 1 of 13
ISSUE/REV.: 1.0 DATE: July 28, 2009

Prepared by	Michele Maris	July 28, 2009
Agreed by	M. Bersanelli LFI Instrument Scientist C.R. Butler LFI Program Manager	2009 July 28th
Approved by	N. Mandolesi LFI Principal Investigator	???

CHANGE RECORD

Issue	Date	Sheet	Description of change	Release
0.1	23th July, 2009	All	First draft issue of document	0.1
0.2	24th July, 2009	All	Spelling corrections, added figures	0.2
0.3	27th July, 2009	All	Added Marco's corrections, presentation and discussion of MC simulations	0.3
0.4	28th July, 2009	All	Complete MC simulations	0.4
1.0	28th July, 2009	All	First issue	1.0

DISTRIBUTION LIST

Recipient	Company/Institute	E-mail address	Sent
N. Mandolesi	INAF-IASF Bologna	reno@bo.iasf.cnr.it	Yes
C. Butler	INAF-IASF Bologna	butler@bo.iasf.cnr.it	Yes
M. Bersanelli	Univ. di Milano	marco.bersanelli@fisica.unimi.it	Yes
A. Mennella	Univ. di Milano	daniele.mennella@fisica.unimi.it	Yes
M. Tomasi	Univ. di Milano	maurizio.tomasi@unimi.it	Yes
M. Balasini	TAS-F Milano	balasini.m@thalesaleniaspace.com	Yes
R. Silvestri	TAS-F Milano	silvestri.r@thalesaleniaspace.com	Yes
P. Leutenegger	TAS-F Milano	leutenegger.p@thalesaleniaspace.com	Yes
M. Miccolis	TAS-F Milano	miccolis.m@thalesaleniaspace.com	Yes
G. Cafagna	TAS-F Milano	cafagna.g@thalesaleniaspace.com	Yes
F. Bertini	ESA	federico.bertini@esa.int	Yes
L. Perez Cuevas	ESA	leticia.perez.cuevas@esa.int	Yes
O. Piersanti	ESA	osvaldo.piersanti@esa.int	Yes
J.P. Chambelland	TAS-F Cannes	jean-philippe.chambelland@thalesaleniaspace.com	Yes
B. Collaudin	TAS-F Cannes	bernard.collaudin@space.alcatel.fr	Yes
P. Rihet	TAS-F Cannes	patrick.rihet@thalesaleniaspace.com	Yes
N. Seville	TAS-F Cannes	norbert.seville@thalesaleniaspace.com	Yes
J.P. Hayet	TAS-F Cannes	jean-pierre.hayet@thalesaleniaspace.com	Yes
A. Gregorio	Univ. di Trieste	anna.gregorio@ts.infn.it	Yes
M. Maris	INAF-OAT Trieste	maris@oats.inaf.it	Yes
A. Zacchei	INAF-OAT Trieste	zacchei@oats.inaf.it	Yes

Contents

LIST OF ABBREVIATIONS

acronym	**Explanation**
LFI	Low Frequency Instrument
TBC	To Be Confirmed
TBD	To Be Defined

1 Applicable and Reference Documents

Applicable Documents

Reference Documents

[RD-1] Maris, M., Maino, D., Burigana, C., Mennella, A., Bersanelli, M., Pasian, F.
The effect of signal digitisation in CMB experiments
A&A, 2004, 777 - 794

2 Scope of the document

This document analyses the degradation of the accuracy of HFI Scientific Thermometers Telemetry as a function of the *quantization step* applied at the output of each thermometer, q_{T}.

Scientific thermometers are those thermometers which are managed by HFI as part of the science telemetry and not as part of House Keeping telemetry.

The HFI team recently identified the need of an increase of the HFI telemetry rate relative to the baseline allocation. The HFI 4K high resolution thermometers are important for LFI for monitoring the reference load temperature The idea behind this exercise is to recover bandwidth in the HFI scientific telemetry by increasing the quantization step applied at the output of these thermometers to gain in Compression Rate, $C_{\mathrm{r,T}}$, for the packets carring such information.

This implies a degradation of the output of such thermometers and so an analysis is needed to asses the maximum level of degradation acceptable for LFI.

This document is a contribution to the action taken at the Telemetry meeting held at MOC July 20^{th}, 2009.

2.1 Limits of Applicability

The analysis refers a simplified case in which the scientific thermometric telemetry is made of time series of temperature measures which are quantized, compressed and sent at ground within the science telemetry.

This is just a simplification of the real process aimed at asses the maximum level of quantization noise acceptable in the output of these sensors in from the LFI point of view. See Sect. 4 for further details on this point.

Table 1: List of symbols

T	temperature measured from the sensor
$q_{\rm T}$	applied quantization at T
$q_{\rm eff,T}$	effective $q_{\rm T}$
$\hat{T}_q$	temperature measured from the sensor after quantization
$V_{\rm T}$, $I_{\rm T}$	voltage and temperature measured from the sensor onboard
$\epsilon_{q,{\rm T}}$, $\epsilon_{q,{\rm V}}$, $\epsilon_{q,{\rm I}}$	quantization error on T, $V_{\rm T}$, $I_{\rm T}$
$G_{\rm T}$	conversion function from $V_{\rm T}$, $I_{\rm T}$ to T (Eq. 1)
$\mathcal{Q}_{\rm T}$	transfer function from quantization errors in $V_{\rm T}$, $I_{\rm T}$ and quantization error in T (Eq. 2)
$\sigma_{\rm noise}$	thermometer instrumental noise rms
$\sigma_{\rm sgn}$	total rms of the thermometer output (including noise and 4K fluctuations)
$f_{\rm smp,HFI}$	thermometers sampling frequency as sent from HFI
$f_{\rm smp,LFI}$	thermometers sampling frequency as downsampled by LFI
$N_{\rm smp}$	downsampling factor
$\epsilon_{\rm PS}$	accuracy in determining the 4K power spectrum from the time serie

3 Requirements for the LFI analysis of 4K thermometers

The key requirements for the LFI analysis of 4K thermometers are [1]:

1. resolution on the temperature scale at 180 Hz better than 1 μK;
2. accuracy in the spectral determination better than 10 $\mu{\rm K}/\sqrt{\rm Hz}$;
3. sampling frequency 2 Hz.

4 Quantization of Thermometric Measures

The analysis in this document assumes that the output of the scientific thermometers are directly sampled, calibrated in temperature, and sent at ground within the science telemetry.

In the real instrument time series of temperature measures from scientific termometers, T_t, are derived from onboard determination of voltage, $V_{{\rm T},t}$, and current, $I_{{\rm T},t}$, for each thermometer which are separately sent at ground (**TBC**) and converted to T_t through a suitable conversion function

$$T_t = G_{\rm T}(I_{{\rm T},t}, V_{{\rm T},t}). \tag{1}$$

The real quantization noise on the thermometric measures, $\epsilon_{q,{\rm T}}$, would be a function of the quantization noises produced by the quantization steps for the $V_{{\rm T},t}$ and $I_{{\rm T},t}$, respectivelly denoted as: $\epsilon_{q,{\rm V}}$ and $\epsilon_{q,{\rm I}}$

$$\epsilon_{q,{\rm T}} = \mathcal{Q}_{\rm T}(\epsilon_{q,{\rm V}}, \epsilon_{q,{\rm I}}, I_{{\rm T},t}, V_{{\rm T},t}), \tag{2}$$

where $\mathcal{Q}_{\rm T}$ is derived from Eq. (1). However we do not know any detail about the $V_{{\rm T},t}$ and $I_{{\rm T},t}$ acquisition, onboard processing and $G_{\rm T}$, which prevents us from carring out a complete and self–consisten analysis.

[1] Terenzi (2009), private communication.

Table 2: Relevant statistics for the L2 thermometer

HFI output		
$f_{\rm smp,HFI}$	180 Hz	
baseline $q_{\rm T}$	0.1	μK
$\sigma_{\rm noise}$	50.3	μK
$\sigma_{\rm 4K}$	415.6	μK
$\sigma_{\rm sgn}$	418.7	μK
signal peak to peak	2508	μK
max S/N 180 Hz	24.93	
LFI postprocessing		
$f_{\rm smp,LFI}$	2 Hz	
Downsampling factor	90	samples
$\sigma_{\rm noise}$	5.3	μK
max S/N 2 Hz	118.26	

Consequently this note is limited at estimating the impact of an assumed level of quantization noise in the temperatures produced by the scientific thermometers. This is equivalent to say that the output of scientific thermometers is processed according to

$$\hat{T}_{t,q} = q_{\rm T} \cdot \text{round}\left(\frac{T_t - \mathcal{O}}{q_{\rm T}}\right) + \mathcal{O}, \tag{3}$$

with $t > 0$ the sampling time of each measure in the time serie, $\mathcal{O}$ a suitable offset. The corresponding quantization noise is defined as

$$\epsilon_{q,\rm T} = \sqrt{\text{var}\left(\hat{T}_{t,q} - T_t\right)}, \tag{4}$$

and in the limit of the *additive noise model* for the quantization noise

$$\epsilon_{q,\rm T} = \frac{q_{\rm T}}{\sqrt{12}}. \tag{5}$$

By using Eq. (5), it will be possible to link the results presented in this note to a real case in which the function $q_{\rm T}$ is specified:

$$q_{\rm eff,T} = \sqrt{12} \cdot \mathcal{Q}_{\rm T}(\epsilon_{q,\rm V}, \epsilon_{q,\rm I}, I_{\rm T}, V_{\rm T}). \tag{6}$$

5 The analyzed data set

We considered as a representative data set the time series for six thermometers acquired by HFI at the OD 62 and provided at the DPC. The most representative and important measures for LFI, are those of P2 and L2. For the scopes of this analysis there are not relevant differences among them. So the analysis is limited at the L2 time series.

A plot of a cycle of the time series is in Fig. 1, while Tab. 2 is a summary of the main statistics of the same signal computed over the whole OD. The evident features are:

Figure 1: A single cycle of L2 thermometer output. For graphical purposes the data have been downsampled of a factor 60.

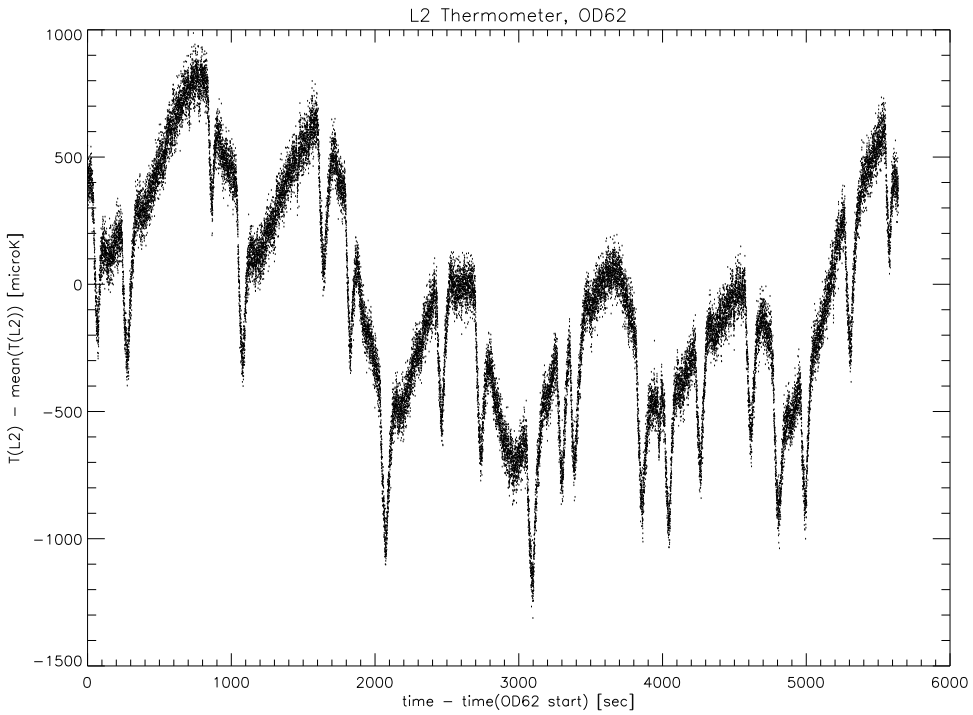

Table 3: Estimated impact of the quantization error on the accuracy of the L2 thermometer telemetry.

q_T	$q_{eff,T}$	σ_{noise}/q_T	$\gamma_{C_{T,T}}$	$\epsilon_{q,T}$	$\epsilon_{q,T}$	σ_{sgn}	σ_{sgn}	Max S/N	Max S/N	ϵ_{PS}
180 Hz	2 Hz		max	180 Hz	2 Hz	180 Hz	2 Hz	180 Hz	2 Hz	
[μK]	[μK]			[μK]	[μK]	[μK]	[μK]			[μK/$\sqrt{\text{Hz}}$]
0.1	0.011	503.00	1.00	0.03	0.003	50.30	5.30	24.93	236.51	3.75
0.5	0.05	100.60	1.20	0.14	0.015	50.30	5.30	24.93	236.51	3.75
1.0	0.11	50.30	1.31	0.29	0.030	50.30	5.30	24.93	236.51	3.75
10.0	1.05	5.03	1.89	2.89	0.304	50.42	5.31	24.89	236.12	3.76
25.0	2.64	2.01	2.30	7.22	0.761	51.01	5.38	24.68	234.11	3.80
50.0	5.27	1.01	2.75	14.43	1.521	53.10	5.60	23.96	227.34	3.96
100.0	10.54	0.50	3.42	28.87	3.043	60.73	6.40	21.62	205.13	4.53

1. the periodical 4K fluctuation, with main periods 940 sec and 6×940 sec due to the sorption cooler cycle and peak–to–peak amplitude of the periodic signal over the whole OD is 2508 μK
2. The while the noise rms is $\sigma_{\rm noise} = 50.3$ μK determined from the residuals after the subtraction of a filtered version of the time series.
3. An enlargement of the figure reveals also that the data are stepped in levels of 0.1 μK likely due to the fact that this is the resolution by which $G_{\rm T}$ is tabulated (**TBC**).

The digitization at point 3 have been neglected and the time series have been processed as if it was not quantized.

6 Analytical Results

We applied Eq. (3) and Eq. (5) for $q_{\rm T} = 0.1$, 0.5, 1, 10, 25, 50 and 100 μK. Those quantization steps are equivalent at $\sigma_{\rm noise}/q_{\rm T} \approx 500$, 100, 50, 5, 2, 1, and 0.5. In all of these cases, the classical approximation for the quantization noise assumes this noise as a non–gaussian, white, additive noise. This model could be safely applied for $q_{\rm T} < \sigma_{\rm noise}$. The quantization noise could be derived from Eq. (5). Indeed, for $q_{\rm T} = 100$ μK some deviation from Eq. (5) is usually expected, but in this explorative exercise the additive model is again good enough to give meaningfull results.

The results of this analysis are reported in Tab. 3 as a function of increasing $q_{\rm T}$ (column 1), where $q_{\rm T} = 0.1$ μK is used as *reference case* given its similarity with the current apparent digitization in the data. Given the thermometers are sampled at $f_{\rm smp,HFI} = 180$ Hz, the LFI team downsamples the time series at $f_{\rm smp,LFI} = 2$ Hz, averaging consecutive groups of $N_{\rm smp} = 90$ samples. For this reason each quantity which is sensitive to downsampling is reported twice in Tab. 3, once at 180 Hz and the other at 2 Hz. After downsampling the quantization noise is reduced of a factor $\sqrt{90}$

$$\epsilon_{q,{\rm T,LFI}} = \frac{q_{\rm T}}{\sqrt{12 N_{\rm smp}}}, \tag{7}$$

(column 5 of the table), which is equivalent to say that at 2 Hz the RMS of the quantization noise is similar to that of a downsampled signal quantized with a quantization step

$$q_{\rm T,LFI} = \frac{q_{\rm T}}{\sqrt{N_{\rm smp}}}, \tag{8}$$

which is also listed in column 2. Of course the quantization could be expressed in terms of $\sigma_{\rm noise}/q_{\rm T}$ which does not depend on the downsampling (colum 3).

The column 4 of the table is a *tentative* estimate of an upper limit for the gain in compression attainable with respect to the current reference case $q_{\rm T} = 0.1$ μK. The gain is defined as the ratio

$$\gamma_{C_{\rm r,T}} = \frac{C_{\rm r,T}(q_{\rm T})}{C_{\rm r,T}(0.1\ \mu{\rm K})}, \tag{9}$$

and in the simple view of a data stream of temperatures directly quantized and compressed by an ideal compressor

$$\gamma_{C_{\rm r,T}} \leq \frac{\log_2(\sqrt{2\pi e}\ \sigma_{\rm sgn}/q_{\rm T})}{\log_2(\sqrt{2\pi e}\ \sigma_{\rm sgn}/0.1\ \mu{\rm K})}, \tag{10}$$

where $\sigma_{\rm sgn}$ is the signal rms including i.e. both the thermal fluctuations and the instrumental noise.

Table 4: Determination of the Main Fourier components of the L2 thermometer fluctuation from the Monte Carlo without quantization. Phases are converted from angular units to time units by scaling for Period/2π.

Component	Period	Amplitude	Phase
$\mathbf{P_1}$	940×6 sec	$\left(270.8 \pm 7 \times 10^{-4}\right)\ \sigma_{\rm noise}$	(-1271.4 ± 0.3) sec
$\mathbf{P_2}$	940 sec	$\left(209.3 \pm 7 \times 10^{-4}\right)\ \sigma_{\rm noise}$	(-348.7 ± 0.1) sec

The expected total noise, the sum in quadrature of the instrumental noise and quantization noise, to be rigorous the exact formula would be

$$\sigma_{\rm noise} = \sqrt{\sigma^2_{\rm noise} + 1.39\epsilon^2_{q,\rm T}}. \tag{11}$$

where the 1.39 coefficient takes in account that 1σ quantization noise does not contain, as for the normal distributed noise, 68.7% of the samples [RD-1].

Assuming both the quantization noise and the instrumental noise act as a white noise (not necessarily gaussian), an estimate of the total uncertainty on the powerspectrum determination, $\epsilon_{\rm PS}$, is derived by dividing the total noise by twice the Nyquist frequency.

$$\epsilon_{\rm PS} = \frac{\sigma^{\rm LFI}_{\rm noise,total}}{\sqrt{f_{\rm smp,LFI}}} \tag{12}$$

which does not depend on the downsampling rate. The goodness of this approximation is the subejct of Sect. 7 and in particular of Sect. 7.3.

7 Monte Carlo simulations of spectral realizations

The spectral accuracy listed in Tab. 3 is just a crude approximation which shall be at least supported by a Monte Carlo simulation. The simulation should be based on a template of the cyclical variation of the L2 thermometer representing the deterministic signal and a simulated noise assumed to be uncorrelated, stationary and normal distributed. In short the MC algorithm is:

1. repeat the template to simulate $N_{\rm cycles}$ cycles of the deterministic part, $T^{\rm template}_t$
2. add to the template the realization of a simulated white noise, n_t, with null mean and unit variance,
$$T^{\rm mc}_t = T^{\rm template}_t + n_t,$$
3. quantize the simulated signal according to Eq. (3) deriving a Monte Carlo realization of the quantized time series for a given $q_{\rm T}$,
4. downsample at 2 Hz the simulated time serie, the resulting time serie is labelled $\hat{T}^{\rm mc}_{t,q}$, $t = 0, 1, 2, \ldots, N_{\rm smp} - 1$ with $N_{\rm smp} = N_{\rm cycles}N_{\rm template}/90$ the number of samples in the time series.
5. The effect of quantization on a single Monte Carlo realization for a given $q_{\rm T}$ is derived by comparing the results with quantization with the results without quantization for a set of predefined metrics.

6. At last mean and variance of the quantization distortion metrics are derived over the whole set of Monte Carlo realizations.

In the remaining part of this discussion we will denote with $X^{\rm mc}_{q=0}$ a quantity X (a metric or a signal) which comes from the Monte Carlo, without to apply the quantization step. In addition the units for the Monte Carlo realizations are normalized to have $\sigma_{\rm noise} = 1$ at the $f_{\rm smp,HFI} = 180$ Hz. The conversion to absolute temperature is obtained by rescaling the simulated data by 50.3 μK according to Tab. 2.

The details of the template derivation are in Sect. 7.1, the uninterested reader could skip such section. Metrics for the evaluation of quantization distortion are in Sect. 7.2. Results from the Monte Carlo are in Sect. 7.3.

7.1 The deterministic template

To have a representative template of cyclical variationf of the L2 signal over a single period, we phase–average more cycles of the original time series and subsequently downsampling the result at 2 Hz. In addition the template time serie have been divided by the noise RMS, so that in this simulation $\sigma_{\rm noise} = 1$ and all of the other quantities are in units of $\sigma_{\rm noise}$.

The power spectrum of the template obtained so far has two components, see Tab. 4, the first labelled P_1 with period 940×6 sec is associated to the cyclical activity of the 6 sorption beds, and the second with period P_1 940 sec is the single bed period. Each component is characterized by its amplitude A and phase ϕ. In the following $A_q = ||{\rm F}_f(\hat{T}_{t,q}, f)/N_{\rm smp}||$ is the amplitude of the sinusoidal component for the frequency f derived from the Fourier transform ${\rm F}_f(.)$ after the quantization of T, while $\phi_q = {\rm argument}({\rm F}_f(\hat{T}_{t,q}, f)/N_{\rm smp})$ the argument for the same Fourier transform. We will put $q = 0$ to denote the same quantities as evaluated before the quantization.

7.2 Metrics on the spectral components determination

To asses the effect on the power spectrum, we analyzed the amplitude A and phase ϕ for the power spectrum main components listed in Tab. 4.

A spectral component is defined by the discrete Fourier transform at its frequency f

$$A_{q,f} e^{i\phi_{q,f}} = \frac{1}{N_{\rm smp}} \sum_{t=0}^{N_{\rm smp}-1} e^{-i2\pi f t/N_{\rm smp}}\, \hat{T}^{\rm mc}_{t,q}, \tag{13}$$

where $\hat{T}^{\rm mc}_{t,q}$ is the outcome of a Monte Carlo realization. In the remaining of the text we will omit the frequency f unless needed for clarity.

The effect on the determination of the amplitudes is evaluated by taking the ratio

$$R_{{\rm A},f}(q) = \frac{A_{q,f}}{A_{q=0,f}}, \tag{14}$$

while for the phases we considered

$$\Delta\phi_{q,f} = \phi_{q,f} - \phi_{q=0,f}. \tag{15}$$

It has to be noted that given the measures are affected by the white noise $A_{q,f}$, $A_{q=0,f}$ $\phi_{q,f}$, $\phi_{q=0,f}$, $R_A(q,f)$ and $\Delta\phi(q,f)$ are stochastic variables whose expectation and variance shall be estimated by the MonterCarlo simulation.

The simulation have been carried out for 1000 Monte Carlo realizations using a wide range of $q_{\rm T}$ values.

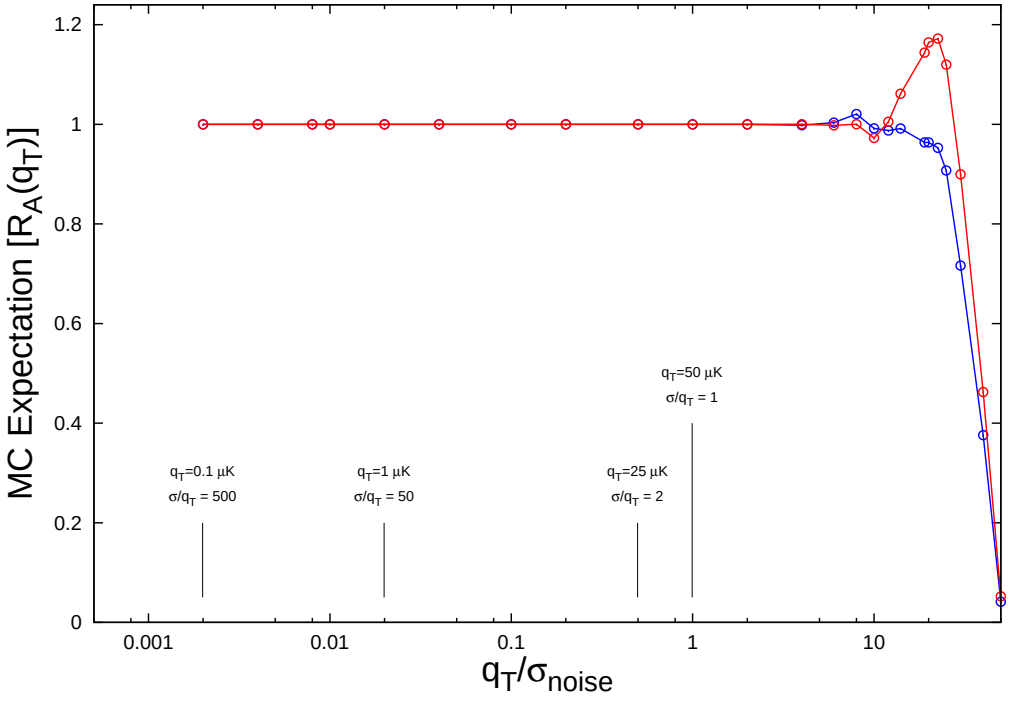

Figure 2: Effect of quantization on the determination of amplitudes by powerspectra from MC simulation. Full–blue line the effect for the P_1 component. Full–red line as before but for the P_2 component.

7.3 Monte Carlo results

We produced 1000 Monte Carlo realizations for $1/500 \leq q_{\rm T}/\sigma_{\rm noise} \leq 50$ extracting the expectations and variances of $R_{{\rm A},f}(q)$ and $\Delta\phi_{q,f}$ for the two main components P_1 and P_2.

Fig. 2 is the expectaion of $R_{\rm A}(q_{\rm T})$ as a function of $q_{\rm T}/\sigma_{\rm noise}$. The variability RMS in the expectation among the Monte Carlo realizations is too small to be appreciated at the scale of the plot. It is evident that as long as $q_{\rm T}$ is less than some $\sigma_{\rm noise}$ the quantization does not affects more than some percent the determination of the amplitude as expected from the theoretical model. But as long as $q_{\rm T}$ becoms too large than $\sigma_{\rm noise}$ there are larger and larger deviations.

According to the noise model for the quantization distortion, since our quantization scheme has zero expectation, the expectation of $A_{q,f}$ would be $A_{q=0,f}$ so that the expectation for the ratio would have to be $R_{\rm A}(q_{\rm T}) = 1$ regardless of $q_{\rm T}$. Instead, from $q_{\rm T} \approx \sigma_{\rm noise}$ there is a bias larger than the variance among Monte Carlo realizations. Indeed in the worst case the RMS of $R_{\rm A}(q_{\rm T})$ less then 10^{-3}.

Fig. 3 represents the error on phases over a single period, as a function of $q_{\rm T}$ with the absolute

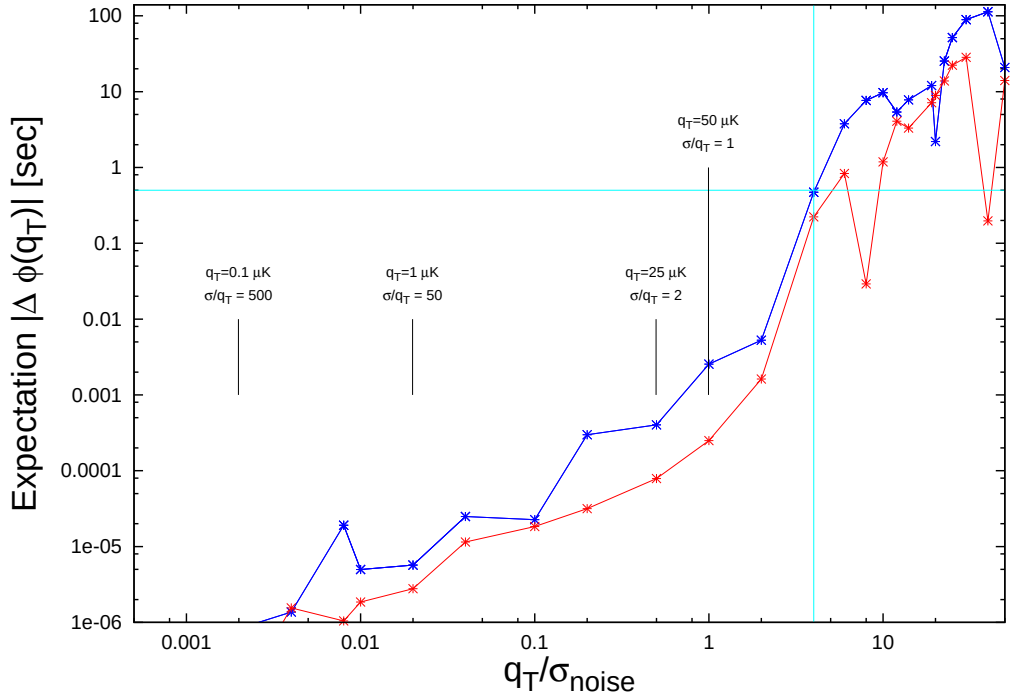

Figure 3: Effect of quantization on the determination of phases by powerspectra from MC simulation. Full–blue line the effect for the P_1 component. Full–red line as before but for the P_2 component. Cian lines denotes where the error of phase becomes comparable to the sampling period for LFI.

error on phases converted from radians to seconds (to be consistent with Tab.4). Even here the variance is too small to be seen on the plot. Quantization has some effect on the determination of phases. for $q_{\rm T}/\sigma_{\rm noise}$ larger than 4 the phase error per cycle becomes comparable to the sampling period 0.5 sec.

Fig 4 is the ratio of variances for quantized and unquatized simulated data among the 1000 Monte Carlos for $R_{\rm A}(q_{\rm T})$ and $\Delta\phi_q$. To scale in absolute units the variances for unquantized data are reported in Tab. 4. The thin black line represents the theoretical espectation for the ratio of variances

$$\frac{\text{variance}\,[X_q]}{\text{variance}\,[X_0]} = 1 + \frac{q_{\rm T}^2}{12\sigma_{\rm noise}^2}, \tag{16}$$

it is evident that the simple expectation from this equation, based on Eq. (11) and Eq. (12), is valid up to $q_{\rm T}/\sigma_{\rm noise} \approx 1.$ and that the same profile is valid for A and ϕ up to $q_{\rm T}/\sigma_{\rm noise} \approx 10$.

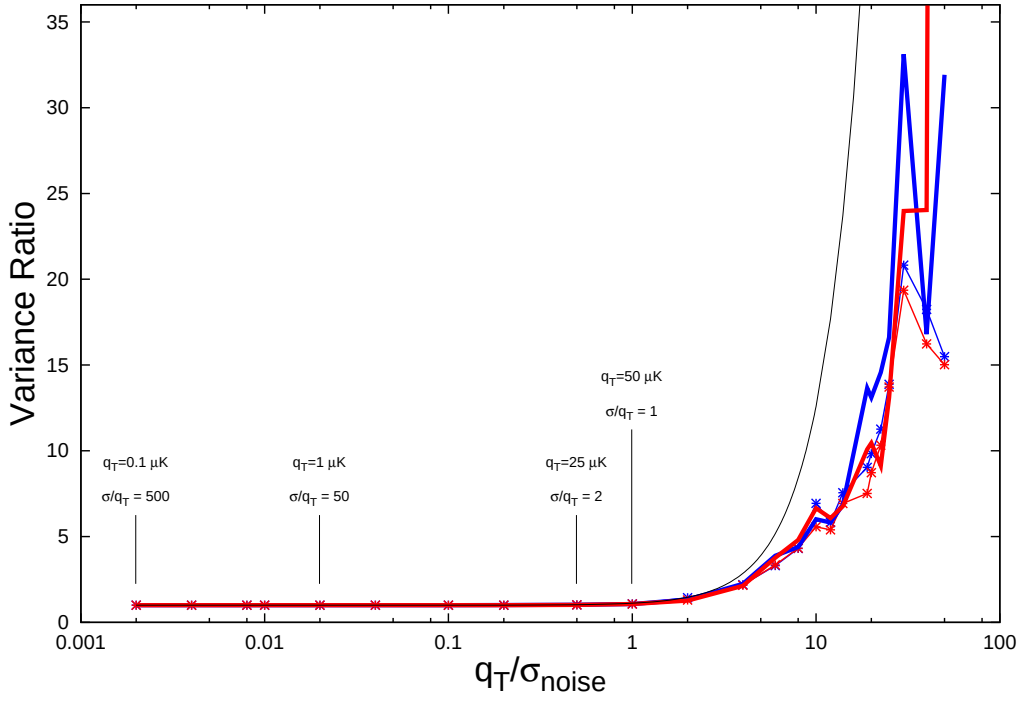

Figure 4: Relative change in variance of Monte Carlo realizzations as a function of q_T. Blue line with stars amplitude of P_1, blue line without symbols argument of P_1. Thick red line argument of P_2, thick blue line argument of P_2. Thin black line the theoretical expectation from Eq. (16).

At last, to derive the $\epsilon_{PS,q}$ in absolute units from the Monte Carlo we applied

$$\epsilon^{mc}_{PS,q} = \sigma^{mc}_{A,q=0}\sigma_{noise}\sqrt{N_{smp}}, \tag{17}$$

with $\sigma^{mc}_{A,q=0}$ the Monte Carlo uncertainty in the amplitude determination reported in Tab. 4, and σ_{noise} the rms of noise in Tab. 2. For the case $q_T = 0$ μK, $\epsilon_{PS,q} = 3.77$ $\mu K/\sqrt{Hz}$ while for $q_T = 1$ μK. $\epsilon_{PS,q} = 3.79$ $\mu K/\sqrt{Hz}$ in line with the crude estimate in Tab. 3.

7.4 Monte Carlo conclusion about Eq. (12)

The crude estimate of $\epsilon_{PS,q}$ from Eq. (12) is a quite good approximation for $q_T \leq \sigma_{noise}$.

8 Discussion, final remarks, conclusions

From this analysis it is evident that it would be possible to push the quantization of the L2 thermometer up to an equivalent q_T of several 10s of μK without to heavily affect the main statistics of the derived thermometric information.

On the other side the requirement 1 is a very stringent one and it allows to increase q_T of at more a factor of 10.

In our simple view for the translation of this increase in q_T into a gain in compression rate, Eq. (10), this probably would represent a modest change in the final data rate. Equivalent to at most some 10% of the output of the L2 thermometer. It is not possible to derive from this ratio a rigorous estimate on how much big would be reduced the telemetry required by HFI since the author has not access to the full information needed to produce such estimate.